2016 International Symposium on Fundamentals of Electrical Engineering
University Politehnica of Bucharest, Romania, June 30 - July 2, 2016

Simulation of surface currents excited by plasma wall-touching kink and vertical modes in tokamak

Calin V. Atanasiu, Leonid E. Zakharov, Karl Lackner, Matthias Hoelzl, Erika Strumberger, Stefan Nicolici

***Abstract*—During plasma disruptions in tokamaks, electric currents are excited in the three-dimensional vessel structures by a plasma Wall Touching Kink Mode (WTKM). These modes are frequently excited during a Vertical Displacement Event (VDE) and cause big sideways forces on the vacuum vessel which are difficult to confront. To understand the plasma disruptions in tokamaks and to predict their effects, realistic simulations of these electric currents are required. In the present paper a flat triangle Finite Element (FE) representation of these surface currents excited in a thin conducting wall of arbitrary three-dimensional geometry is described. Our wall model covers both eddy currents, excited inductively, and source/sink currents due to current sharing between the plasma and the wall.**

***Index Terms*—Fusion plasma, Tokamak, MHD instabilities, Plasma disruptions**

I. Introduction

EVEN if disruptions in tokamaks are known since 1963, some aspects of them remain unknown. The Wall Touching Kink Modes (WTKM) were discovered at Joint European Tokamak (JET) in 1996 [1]. Due to the presence of an electric contact with the wall, the plasma is unstable. The surface currents excited by the WTKM and shared with the wall are called Hiro currents [2]. It has been found that free boundary Magneto Hydro Dynamic (MHD) modes (an $m/n = 1/1$ kink mode) are generating the currents shared by the plasma with the wall during tokamak disruptions [3]. Vertical Displacement Events (VDE) on JET and recent measurements of Hiro currents on Experimental Advanced Superconducting Tokamak (EAST) in 2012 have proven this [3]. It has been found also from both theory and JET, EAST experimental measurements that the galvanic contact of the plasma with the wall is critical in disruption [4], [5]. At the same time it has been proven that the thin wall approximation is sufficient (i.e., the real volume current distribution in the wall can be replaced by a current layer along the plasma-facing surface), but for simulating the plasma-wall interaction during disruption, the reproduction of 3D structure of the wall is important.

C. Atanasiu is with the National Institute for Laser, Plasma and Radiation Physics 077125 Magurele-Bucharest, Romania, email: cva@ipp.mpg.de.

L. Zakharov is with the LiWFusion, P.O. Box 2391, Princeton, NJ 08543, USA.

K. Lackner, M. Hoelzl and E. Strumberger are with the Max Planck Institute for Plasma Physics, Boltzmannstr. 2, 85748 Garching, Germany.

S. Nicolici is with the Nuclear Engineering Technology Center, 077125 Bucharest-Magurele, Romania.

This work has been partially supported by US DoE contract no. DE-AC02-09- CH11466 and partially carried out out within the framework of the EUROfusion Consortium and has received funding from the Euratom research and training programme 2014-2018 under grant agreement no. 633053. The views and opinions expressed herein do not necessarily reflect those of the European Commission.

978-1-4673-9575-5/16/$31.00 ©2016 IEEE

II. Formulation of the problem

A. Surface current components in the thin wall

According to the Helmholtz decomposition theorem, for the total surface current $d\mathbf{j}$ (d being the wall thickness) two components can be defined: (a) one is a divergence free surface current $\mathbf{i}$ and (b) the second one is proportional with $-\nabla\Phi^S$, with Φ^S the source/sink potential, a surface function. In order to describe the current sharing between the plasma and the wall, the second surface current component has a potentially finite divergence. Thus,

$$d\mathbf{j} = \mathbf{i} - \sigma d\nabla\Phi^S, \quad \mathbf{i} \equiv \nabla I \times \vec{n}, \tag{1}$$

where, I is the stream function of the divergence free component $\mathbf{i}$ ($\nabla \cdot \mathbf{i} = 0$) [7], [8], $\vec{n}$ is the external unit normal vector to the wall, σd is the surface wall conductivity and $-\sigma d\nabla\Phi^S$ is the source/sink current.

The source/sink surface current $-\sigma d\nabla\Phi^S$ is obtained from the sharing of the electric current between the plasma and the wall. Such current can be determined from the following equation

$$\nabla \cdot (\sigma d\nabla\Phi^S) = -(\mathbf{j} \cdot \vec{n}) = j_\perp, \tag{2}$$

where $j_\perp$ is the density of the current coming from/to the plasma. It is a galvanic source for the surface currents on the wall. We have considered $j_\perp$ as positive for a current flowing from the plasma to the wall.

B. Energy principle applied to the surface currents in a thin wall

Φ^S can be obtained by minimizing the functional $\mathcal{W}^S$ [5], [6]

$$\begin{aligned}\mathcal{W}^S &= \frac{1}{2}\int \Big[\sigma d(\nabla\Phi^S)^2 - 2j_\perp\Phi^S\Big]dS \\ &- \frac{1}{2}\oint \Phi^S\sigma d[(\vec{n}\times\nabla\Phi^S)\cdot d\mathbf{l}],\end{aligned} \tag{3}$$

while $\mathbf{i} = \nabla I \times \vec{n}$ can be obtained from the following energy functional $\mathcal{W}^I$ [6], [7], [9], [10], [8], [12], [13]

$$\begin{aligned}\mathcal{W}^I &= \int \Big[\frac{1}{2}\frac{\partial(\mathbf{i}\cdot\mathbf{A}^I)}{\partial t} + \frac{1}{2\sigma d}|\nabla I|^2 \\ &+ \mathbf{i}\cdot\frac{\partial\mathbf{A}^{ext}}{\partial t}\Big]dS - \oint(\Phi^E - \Phi^S)\frac{\partial I}{\partial l}dl,\end{aligned} \tag{4}$$

The first integral, a surface integral, is taken along the wall surface, while the second one, a contour integral, is taken along the edges of the conducting surfaces. Φ^E is some electrical potential applied to the wall. In practical cases,

there is no source/sink of the current through the edges of the wall surface and thus the contour integral vanishes. $\mathbf{A}^I$ is the vector potential of the current $\mathbf{i}$, while $\mathbf{A}^{ext}$ is the vector potential generated by the plasma, external coils and source/sink currents.

III. Numerical results

In our FE approach, Φ^S and I are assumed to be linear and C^0. So, both are linear within each triangle and neighboring triangles share the values on the nodes. The minimization of the quadratic forms Eqs. (3, 4) gives a linear system of equations with symmetric positively defined matrices which has been solved using the Cholesky decomposition [6].

In our calculations we have solved Eq. (3) for $\mathcal{W}^S$ with given $j_\perp$ as r.h.s. and Eq. (4) for $\mathcal{W}^I$ with given $\mathbf{A}^{ext}$ as r.h.s. The following boundary conditions have been considered: for Φ^S Neumann boundary conditions on the wall and holes boundaries

$$\frac{\partial \Phi^S}{\partial n_s} = 0, \tag{5}$$

and for I Dirichlet boundary conditions with different constant values on the wall boundary and hole boundaries [10], [11]

$$\frac{\partial I}{\partial l} = 0, \tag{6}$$

where $\mathbf{n}_s$ ($\mathbf{n}_s \neq \mathbf{n}$) is the normal to the contours in the plane of the considered wall triangle, while l is the line coordinate of the boundaries.

As an example of source/sink currents calculation a ITER wall configuration has been considered. For this ITER wall configuration, a FE discretization mesh with 11223 vertexes and 21744 triangles has been considered. The generation of the matrix and its Choleski decompositions take about 15s, after this, the solution of the equation takes several seconds for given $j_\perp$ distributions. Two localized source (red) and sink (blue) areas are considered in Fig. 1. For simplicity only, we have considered σd=1, but variable wall thickness d and conductivity σ can be taken also into account. The distribution of source/sink potential Φ^S and of the source/sink current $-\sigma d \Phi^S$ over the wall surface is given in Fig. 2.

IV. Verification and validation of numerical simulations with an analytical solution

To check the accuracy of our source/sink code, an analytical example with pure homogeneous Neumann B.C. has been developed. This example satisfies the existence condition:

$$\int_{\partial\Omega} \frac{\partial \Phi^S}{\partial n} dl = -\int_{\Omega} j_\perp dS = 0,$$
$$\Omega = \Omega_e \setminus \Omega_i, \quad \partial\Omega = \Gamma_e \cup \Gamma_i, \tag{7}$$

where Ω_e is the domain of the wall, Ω_i is the domain of the hole, while Γ_e and Γ_i are the boundaries of the wall and hole respectively.

As domain for the analytical test problem, a toroidal wall with R its big radius, with elliptical cross-section a/b and a central hole has been considered (Fig. 3).

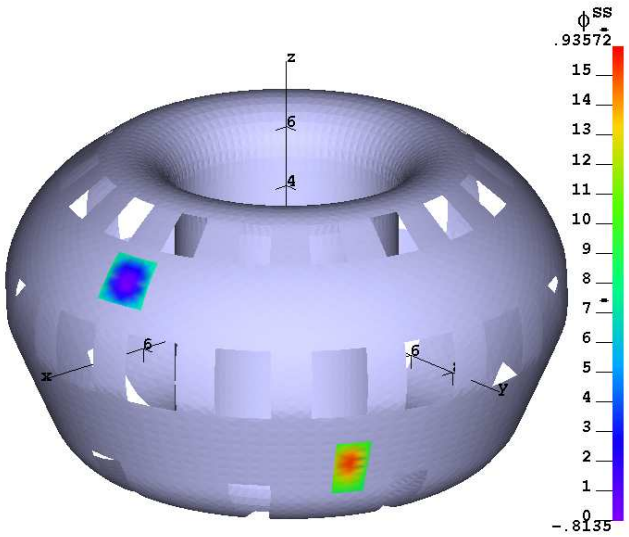

Fig. 1. Distribution of $j_\perp$ in the wetting zones of a ITER wall configuration.

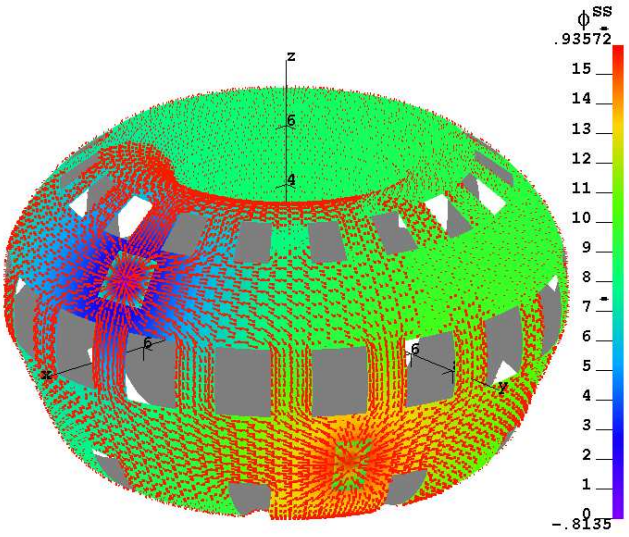

Fig. 2. Distribution of the Φ^S and $-d\nabla\Phi^S$ solutions for a ITER wall configuration with the $j_\perp$ distribution given in Fig. 1 .

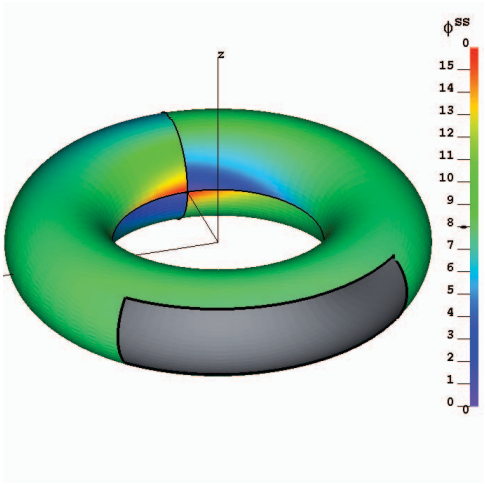

(a)

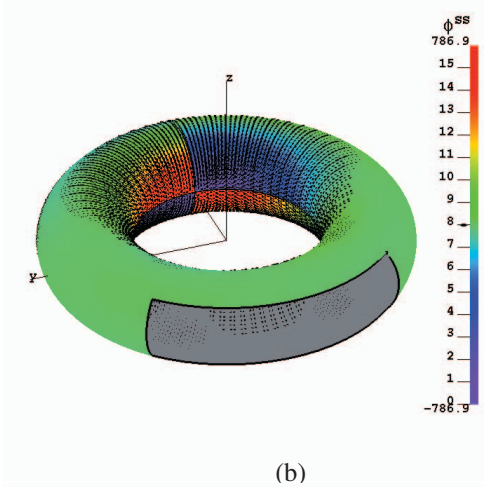

(b)

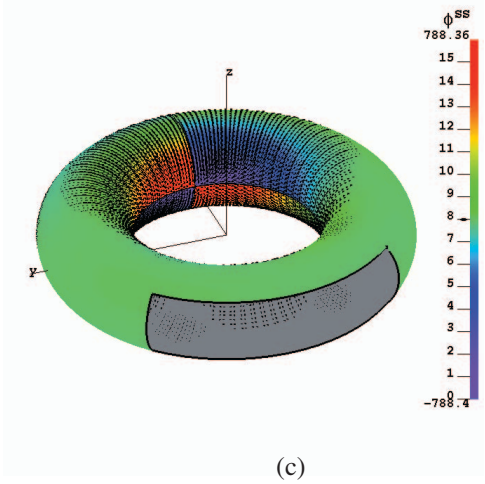

(c)

Fig. 3. Analytical model of a wall with high resolution (64x64x4 triangles) ($a = b$, $R/a = 3/1$) with a poloidal and toroidal cuts and a hole in the low field side surface. (a) The input value $j_\perp$. (b) The analytical Φ^S. (c) Φ^S based on numerical solution. The value of the relative inaccuracy is 0.001.

Assuming for simplicity $\sigma d \equiv 1$, and considering a curvilinear coordinate system u, v, ($u \equiv \phi$, the toroidal coordinate, and $v \equiv \theta$, the poloidal coordinate) Eq. (2) can be written as

$$\frac{1}{h_u h_v}\left[\frac{h_v}{h_u}\frac{\partial^2 \Phi^S}{\partial u^2} + \frac{\partial}{\partial v}\left(\frac{h_u}{h_v}\right)\cdot\frac{\partial \Phi^S}{\partial v} + \frac{h_u}{h_v}\frac{\partial^2 \Phi^S}{\partial v^2}\right] = j_\perp(u,v), \tag{8}$$

with h_u and h_v the Lamé coefficients. For Φ^S, the following dependence has been deduced

$$\begin{aligned}\Phi^s(u,v) &= \left\{\frac{1}{5}u^5 + uu_0u_1u_2u_I - \frac{1}{4}u^4(u_0+u_1+u_2+u_I)\right.\\ &+ \frac{1}{3}u^3(u_2u_I + u_1(u_2+u_I) + u_0(u_1+u_2+u_I))\\ &- \left.\frac{1}{2}u^2(u_1u_2u_I + u_0(u_2u_I + u_1(u_2+u_I)))\right\}\\ &\times \left\{\frac{1}{5}v^5 + vv_0v_1v_2v_J - \frac{1}{4}v^4(v_0+v_1+v_2+v_J)\right.\\ &+ \frac{1}{3}v^3(v_2v_J + v_1(v_2+v_J) + v_0(v_1+v_2+v_J))\\ &- \left.\frac{1}{2}v^2(v_1v_2v_J + v_0(v_2v_J + v_1(v_2+v_J)))\right\}. \end{aligned}\tag{9}$$

where different u and v values are explained in Fig. 4. In the same figure, the distribution of Φ^S isolines in the multiply connected domain $\Omega(u,v)$ is given.

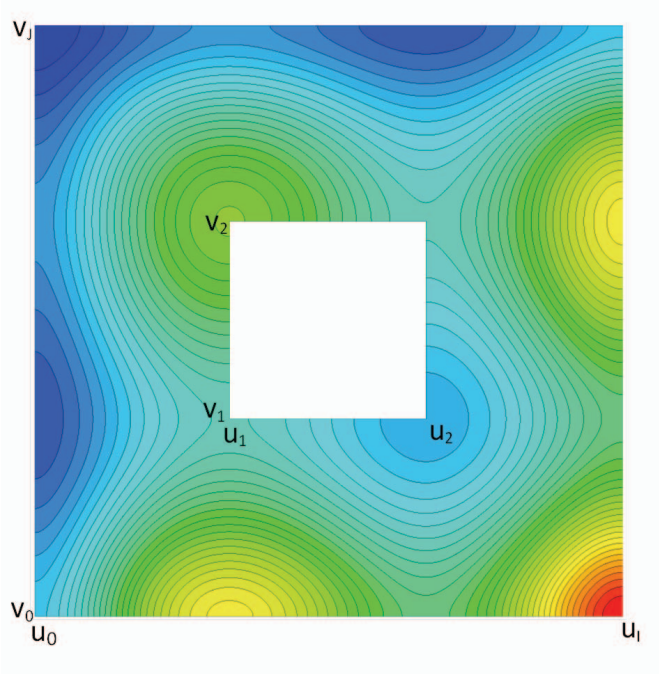

Fig. 4. Constant $\Phi^S(u,v)$ lines (given by Eq. (9) and satisfying pure Neumann boundary conditions on wall and hole boundaries.

A comparison of the analytical and numerical solutions for a high resolution mesh (64x64x4 triangles) on the wall surface is given in Figs. 3b,3c.

In the next Table, different FE discretization levels of the wall geometry (Fig. 3) have been considered.

No. of triangles	Relative accuracy
64 x 64 x 4	0.001
32 x 32 x 4	0.003
16 x 15 x 4	0.015

V. Conclusion

The two surface current components and the surface current circuit equations in the thin wall approximation have been mathematically rigorous formulated. The divergence-free eddy and the source/sink currents are represented by the same model of a uniform current density inside each triangle of our Finite Element representation of the wall surface.

In order to allow self-consistent simulations of plasma dynamics and plasma-wall interactions in tokamak disruptions, we intend to develop, as a next step, a realistic representation of the wetting zone and to interface the wall current codes with plasma simulation codes, such as STARWALL [8], [12], [13] and JOREK [14], [15], [16].

Acknowledgment

The authors express their appreciation to the late Academician Vitaly Dmitrievich Shafranov from the I.V. Kurchatov Institute, one of the greatest plasma theoretician in the field.

References

[1] R. Litunovski. "The observation of phenomena during plasma disruption and the interpretation of the phenomena from the point of view of the toroidal asymmetry of forces", JET Internal Report Contract No. JQ5/11961 1995.

[2] L.E. Zakharov, "The theory of the kink mode during the vertical plasma disruption events in tokamaks", Phys. Plasmas 15, 2008, pp. 062507-1 - 062507-8.

[3] L.E. Zakharov, S. A. Galkin, S.N. Gerasimov and JET-EFDA Contributors, "Understanding disruptions in tokamaks", Phys. Plasmas 19, 2012, 055703-1 - 055703-13 .

[4] L.E. Zakharov, X. Li, "Tokamak magneto-hydrodynamics and reference magnetic coordinates for simulations of plasma disruptions", Phys. Plasmas 22, 2015, pp. 062511-1 - 062511- .

[5] L.E. Zakharov, H. Xiong, D. Hu, X. L, C.V. Atanasiu, Hiro currents: physics and a bit of politics, Theory and Simulation of Disruptions Workshop, July 17-19, 2013, PPPL, Princeton NJ, USA.

[6] L.E. Zakharov, C.V. Atanasiu, K. Lackner, M. Hoelzl, and E. Strumberger "Electromagnetic thin-wall model for simulations of plasma walltouching kink and vertical modes", Journal of Plasma Physics 81, 2015, pp. 515810610-1 - 515810610-22.

[7] C.V. Atanasiu and L.E. Zakharov, "Response of a partial wall to an external perturbation of rotating plasma", Phys. Plasmas 20, 2013, pp. 092506-1 - 092506-11.

[8] P. Merkel, C. Nührenberg, and E. Strumberger, "Resistive Wall Modes of 3D Equilibria with Multiply-connected Walls". 31 st. EPS Conference on Plasma. Physics. Europhys. Conf. Abstrats 28G, P1.208 (2004)

[9] C.V. Atanasiu, S. Günter, K. Lackner, and L.E. Zakharov, "Linear tearing modes calculation for diverted tokamak configurations", Phys. Plasmas 12, 2004, pp. 5580-5594.

[10] C.V. Atanasiu, A. Moraru and L.E. Zakharov, "Influence of a Nonuniform Resistive Wall on the RWM Stability in a Tokamak", American Physical Society Plasma 51st Annual Meeting, Atlanta, USA, 2-6 November 2009.

[11] C.V. Atanasiu, A. Moraru and L.E. Zakharov, "MHD Modeling in Diverted Tokamak Configurations", 7th ATEE-2011 International Symposium, May 12-14, 2011, Bucharest, Romania.

[12] P. Merkel, M. Sempf. "Feedback Stabilization of Resistive Wall Modes in the Presence of Multiply connected Wall Structures". (TH/P3-8) Procs. 21st IAEA Fusion Energy Conference, Chengdu, China, 2006.

[13] P. Merkel, E. Strumberger, "Linear MHD stability studies with the STARWALL code", arXiv:1508.04911 (2015).

[14] G.T.A. Huysmans and O. Czarny, "MHD stability in X-point geometry: simulation of ELMs", Nucl. Fusion 47, 2007, pp. 659-666.

[15] M. Hoelzl, P. Merkel, G.T.A. Huysmans, E. Nardon, R. McAdams, and I. Chapman "Coupling the JOREK and STARWALL Codes for Non-linear Resistive-wall Simulations", Journal of Physics: Conference Series, 401, 2012, pp. 012010-1 - 012010-8 .

[16] M. Hoelzl, G.T.A. Huijsmans, P. Merkel, C.V. Atanasiu, K. Lackner, E. Nardon, K. Aleynikova, F. Liu, E. Strumberger, R. McAdams, I. Chapman and A. Fil, Journal of Physics: Conference Series 561, 12/2014, pp. 012011-1 - 012011-10 .